

Effective Medium Theory of Semiflexible Filamentous Networks

Moumita Das,^{1,*} F. C. MacKintosh,² and Alex J. Levine^{1,3}

¹*Department of Chemistry, University of California, Los Angeles, California 90095, USA*

²*Department of Physics and Astronomy, Vrije Universiteit, Amsterdam, The Netherlands*

³*California Nanosystems Institute, University of California, Los Angeles, California 90095, USA*

(Received 10 August 2006; published 18 July 2007)

We develop an effective medium approach to the mechanics of disordered, semiflexible polymer networks and study the response of such networks to uniform and nonuniform strain. We identify distinct elastic regimes in which the contributions of either filament bending or stretching to the macroscopic modulus vanish. We also show that our effective medium theory predicts a crossover between affine and nonaffine strain, consistent with both prior numerical studies and scaling theory.

DOI: [10.1103/PhysRevLett.99.038101](https://doi.org/10.1103/PhysRevLett.99.038101)

PACS numbers: 87.16.Ka, 62.20.Dc, 82.35.Pq

Semiflexible polymer networks form a distinct class of gels whose mechanics is important for both biophysical and materials research. These cross-linked polymer networks differ substantially from the flexible polymer gels and rubbers [1] due to the rigidity of the individual polymers [2,3]. Because the thermal persistence length of the constituent filaments is much longer than the typical distance between cross-links, these materials can store elastic strain energy in both stretching and bending the filaments. The cytoskeleton, a complex assembly that includes stiff filamentous proteins present in most eukaryotic cells, is an especially common example of such a semiflexible network [4]. Such networks dominate the mechanical properties of the cytosol and are at the heart of cellular force production and morphological control.

Theoretical studies of the elastic response of randomly cross-linked, stiff, filamentous networks have recently uncovered a surprising crossover between distinct mechanical regimes of these semiflexible networks [5,6]. For given filament elastic parameters, there is a transition from strain energy storage in filament-stretching modes at higher network densities to filament-bending modes in sparser networks. This transition is accompanied by a change in the geometry of the deformation field over mesoscopic lengths. At higher densities, the network deforms affinely as expected from continuum elasticity theory, while at lower densities, where the elastic energy is stored in bending modes, the network deformation field is nonaffine over mesoscopic distances. Recent experiments [7,8] support the existence of this affine (A) to nonaffine (NA) crossover. However, a fundamental understanding of the relation of the network architecture and individual filament mechanics to the collective elasticity of the network remains elusive, and prior theoretical work has been primarily numerical.

In this Letter, we develop an analytical model of the mechanical response of two-dimensional, disordered, semiflexible networks. We introduce a mean-field or effective medium theory of the system that allows us to calculate the elastic response of the system to uniformly

imposed as well as wave number-dependent strain fields. From this mechanical response, we identify an A-NA crossover and obtain a phase diagram of the system showing the regimes of affine and nonaffine behavior. Our study also demonstrates the presence of a length scale controlling the A-NA crossover that corresponds well with prior results from simulation and scaling theory [5].

We study a model two-dimensional system constructed as follows. We arrange infinitely long filaments in the plane of a two-dimensional hexagonal lattice so that at each lattice point three filaments cross. In this way, each lattice point is connected to its nearest neighbor by a single filament. The network is shown in Fig. 1. The filaments are given an extensional spring constant α and a bending modulus κ . The cross-links at each lattice site do not constrain the angle between the crossing filaments. We introduce finite filament length L into the system by cutting bonds with probability $1 - p$, where $0 < p < 1$, with no spatial correlations between these cutting points. This gen-

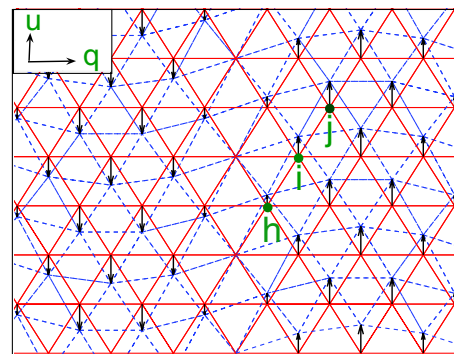


FIG. 1 (color online). Schematic figure of the filament network. The solid red lines represent the undeformed filament network, while the dashed blue lines show the deformation field having wave vector \mathbf{q} and displacement amplitude \mathbf{u} (shown in the upper left corner of the figure). The black arrows show the displacement field at each lattice point. This perfect lattice is disordered by making randomly placed cuts in the infinitely long filaments. These are not shown.

erates a broad distribution of filament lengths with a finite average $\langle L \rangle$, while introducing quenched disorder. We then study the mechanical response of this disordered network in the linear response regime. The main assumption in our theory is that the depleted network has the same mechanical response as a uniform network with effective elastic constants α_m and κ_m . These are determined by requiring that strain fluctuations produced in the original, ordered network by randomly cutting the filaments have zero average. Here we do not explicitly consider thermal fluctuations, whose role in determining the longitudinal compliance of filaments has been discussed before [9]. These thermal effects can be incorporated in the present model through a renormalized parameter α [5].

The elastic energy of the strained network, arising from bending and stretching of the constituent filaments, can be written in terms of the displacement vector \mathbf{u}_i at each lattice site i . To quadratic order in \mathbf{u} , the stretching (E_s) and bending (E_b) energies are

$$E_s = \frac{1}{2} \alpha \sum_{\langle ij \rangle} (\mathbf{u}_{ij} \cdot \hat{\mathbf{r}}_{ij})^2, \quad (1)$$

$$E_b = \frac{1}{2} \kappa R^{-2} \sum_{\langle hij \rangle} (\mathbf{u}_{ih} \times \hat{\mathbf{r}}_{ij} - \mathbf{u}_{ij} \times \hat{\mathbf{r}}_{ih})^2, \quad (2)$$

where R is the lattice constant, $\hat{\mathbf{r}}_{ij}$ is a unit vector directed from the i th to the j th equilibrium lattice site, and \mathbf{u}_{ij} is the difference in the strain field between those lattice sites.

It is now simple to determine the collective elastic properties of the perfect lattice; doing so for the disordered lattice generated by randomly cutting the filaments is less trivial. We determine the spring constant and bending modulus of a spatially uniform effective system [10] that reproduces the mechanics of our disordered system in an average sense as described below.

We first apply a uniform dilation to the uniform system with spring constant α_m so that all bonds are stretched by $\delta\ell$. There is no bending deformation. If we now replace a single filament segment connecting points (say) i and j (see Fig. 1) by one of spring constant α' , the virtual force needed to the fix positions of i and j is $f = \delta\ell(\alpha_m - \alpha')$. If f were applied to the same segment in the unstrained network, the resulting change in length would be $f/(\alpha_m/a^* - \alpha_m + \alpha')$, where a^* ($0 < a^* < 1$) is a network material parameter that includes the contribution of the elasticity of the entire network. It may be written in terms of the dynamical matrix $\mathbf{D}(q)$ as

$$a^* = \frac{1}{3} \sum_q \text{Tr}[\mathbf{D}_s(q) \cdot \mathbf{D}^{-1}(q)], \quad (3)$$

where the sum is over the first Brillouin zone. Here $\mathbf{D}(q) = \mathbf{D}_s(q) + \mathbf{D}_b(q)$, where $\mathbf{D}_{s,b}(q)$ define the stretching and bending contributions, respectively, to the full dynamical matrix and are given by

$$\mathbf{D}_s(q) = \alpha_m \sum_{\langle ij \rangle} [1 - e^{-iq \cdot \hat{\mathbf{r}}_{ij}}] \hat{\mathbf{r}}_{ij} \hat{\mathbf{r}}_{ij}, \quad (4)$$

$$\begin{aligned} \mathbf{D}_b(q) = & \kappa_m R^{-2} \sum_{\langle ij \rangle} \{4[1 - \cos(\mathbf{q} \cdot \hat{\mathbf{r}}_{ij})] - [1 - \cos(2\mathbf{q} \cdot \hat{\mathbf{r}}_{ij})]\} \\ & \times (\mathbf{I} - \hat{\mathbf{r}}_{ij} \hat{\mathbf{r}}_{ij}), \end{aligned} \quad (5)$$

with \mathbf{I} the unit tensor and the sums are over nearest neighbors [10]. Note that, for small q , $\mathbf{D}_b \sim q^4$ and $\mathbf{D}_s \sim q^2$ have the expected wave number dependencies for bending and stretching.

From linearity, the extra displacement δu of the segment ij due to the change in that filament segment's spring constant in the dilated network is the same as its extension in response to the force f applied to it. Therefore, this additional displacement or ‘‘fluctuation’’ is

$$\delta u = \frac{(\alpha_m - \alpha') \delta\ell}{\alpha_m/a^* - \alpha_m + \alpha'}. \quad (6)$$

We now average this extra displacement over the ensemble of possible filament substitutions, with the statistical distribution of longitudinal spring constants:

$$P(\alpha') = p\delta(\alpha - \alpha') + (1 - p)\delta(\alpha'), \quad (7)$$

where $1 - p$ is the probability of a cut bond and $\delta(\dots)$ is the Dirac delta function. To determine the elastic properties of the effective medium, we adjust the medium spring constants α_m so that $\langle \delta u \rangle = 0$; i.e., the lattice displacement in our spatially homogeneous effective medium material is identical to the average displacement in the spatially heterogeneous disordered material.

Using this procedure, we find a spatially homogeneous effective medium having spring constant α_m given by

$$\frac{\alpha_m}{\alpha} = \begin{cases} \frac{p-a^*}{1-a^*} & \text{if } p > a^*, \\ 0 & \text{if } p \leq a^*. \end{cases} \quad (8)$$

The contribution of network bending to the effective medium spring constant (which is proportional to the collective shear modulus) arises only through the effect of the bending modulus on a^* in Eqs. (3)–(5).

To determine how the shear modulus depends on the average filament length, we note that the mean filament length is $\langle L \rangle = pR(2 - p)/(1 - p)$. We plot in Fig. 2 using the solid symbols the effective medium spring constant as a function of the mean filament length measured in units of R .

We now consider the response of the network to a q -dependent strain as depicted in Fig. 1. We modify both the bending modulus and spring constant of one filament spanning lattice sites h , i , and j so that $\kappa_m \rightarrow \kappa'$, $\alpha_m \rightarrow \alpha'$, and compute the virtual force and torque needed to maintain the position of site i in the middle of this triad of lattice sites (Fig. 1). Using these forces and linearity, we compute the displacement of the i th site in response to the elastic constant substitution made above. We find that the dis-

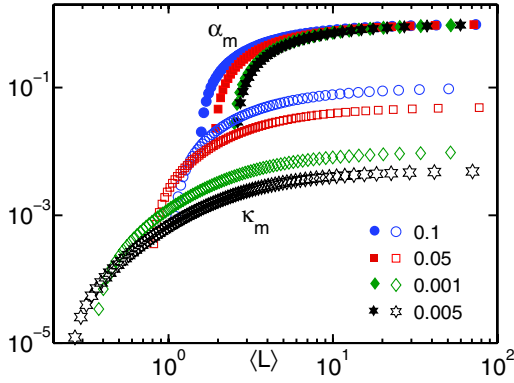


FIG. 2 (color online). The effective medium spring constant α_m (solid symbols) and bending constant κ_m (open symbols) with the average filament length $\langle L \rangle$ (legend shows different values of κ , with $\alpha = 1$).

placements along the filament ($\delta\ell_{\parallel}$) and perpendicular to it ($\delta\ell_{\perp}$) are given by

$$\delta\ell_{\parallel} = \frac{(\alpha_m - \alpha')(\mathbf{u}_{ij} + \mathbf{u}_{ih}) \cdot \hat{\mathbf{r}}_{ij}}{2(\alpha_m/a^* - \alpha_m + \alpha')}, \quad (9)$$

$$\delta\ell_{\perp} = \frac{(\kappa_m - \kappa')(\mathbf{u}_{ij} + \mathbf{u}_{ih}) \cdot (\hat{\mathbf{z}} \times \hat{\mathbf{r}}_{ij})}{\kappa_m/b^* - \kappa_m + \kappa'},$$

where a^* is defined in Eq. (3) and the analogous quantity b^* is defined by

$$b^* = \frac{1}{3} \sum_q \text{Tr}[\mathbf{D}_b(q)\mathbf{D}^{-1}(q)] \quad (10)$$

using the same sum over wave vectors as in Eq. (3). For filaments on a triangular lattice interacting via cross-links that do not apply torques, the stretching and bending modes are orthogonal to first order in deformations.

We now average these displacements over the disorder, and, to find the effective medium elastic constants, we demand that the disorder-averaged displacements $\langle\delta\ell_{\parallel}\rangle$ and $\langle\delta\ell_{\perp}\rangle$ vanish. The probability distribution for α' is given by Eq. (7), but a nonzero value of the bending modulus at site i requires the presence of *both* filament segments on either side of that site so that

$$P(\kappa') = p^2\delta(\kappa - \kappa') + (1 - p^2)\delta(\kappa'). \quad (11)$$

Since we consider uncorrelated distributions of the bending and elastic constants, we find the effective medium elastic constants α_m and κ_m by solving Eq. (9) for $\langle\delta\ell_{\parallel}\rangle = \langle\delta\ell_{\perp}\rangle = 0$ independently to arrive at

$$\frac{\alpha_m}{\alpha} = \begin{cases} \frac{p-a^*}{1-a^*} & \text{if } p > a^*, \\ 0 & \text{if } p \leq a^*, \end{cases} \quad (12)$$

$$\frac{\kappa_m}{\kappa} = \begin{cases} \frac{p^2-b^*}{1-b^*} & \text{if } p > \sqrt{b^*}, \\ 0 & \text{if } p \leq \sqrt{b^*}. \end{cases} \quad (13)$$

Figure 2 shows the effective medium values of α_m (solid symbols) and κ_m (open symbols) as a function of $\langle L \rangle$ for different values of bending rigidity κ , at a fixed value of $\alpha = 1$. The unit of length is the lattice constant R (set to unity), and the energy scale is arbitrary.

There are three length scales in the system: (i) the average length of filaments $\langle L \rangle$, (ii) a length $l_b = (\kappa/\alpha)^{1/2}$ associated with the relative ease of filament stretching to bending, and (iii) the mean distance between cross-links, which to a good approximation is R [11]. We present a mechanical phase diagram of our system spanned by $\langle L \rangle$ and l_b in Fig. 3 that shows the regimes corresponding to zero and finite values of κ_m and α_m . Generically, for long enough filaments, the system has finite collective extension and bending moduli. As the mean filament length is reduced, the collective shear modulus vanishes at the rigidity percolation transition [10,12,13]. We also find a new rigid phase ($\alpha_m > 0$) that has a vanishing bending modulus κ_m [14]. We further note that the lower range in l_b corresponds to nonthermal systems in which the distance between cross-links is large compared with the molecular scale (i.e., at low volume fraction) but that, with thermal effects, one effectively goes to higher l_b .

The collective elastic properties of the effective medium can be calculated from the stored energy density \mathcal{E} under a given network strain. For a strain field of the form $\mathbf{u} = R\gamma \cos(\mathbf{q} \cdot \mathbf{x})\hat{\mathbf{z}} \times \hat{\mathbf{q}}$, the shear G_{eff} and bending moduli K_{eff} can be extracted as the coefficients of the q^2 and q^4 terms of $\langle\mathcal{E}\rangle/\gamma^2$, where the angle brackets imply an average of the direction of \mathbf{q} with respect to the underlying lattice. G_{eff} is proportional to α_m alone, while K_{eff} is a function of κ_m and α_m .

In Fig. 4, we plot the effective medium shear and bending moduli as a function of $\langle L \rangle$. Motivated by earlier work [5] on the A-NA transition, we have rescaled $\langle L \rangle$ by $\lambda = R(R/l_b)^z$, with $z = 1/4$. A comparison of G_{eff} in this figure

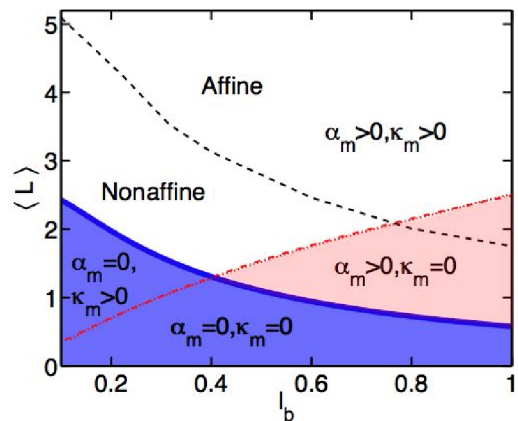


FIG. 3 (color online). The effective medium mechanical phase diagram spanned by $\langle L \rangle$ and l_b . The thick solid line marks the rigidity percolation transition where the material acquires a finite shear modulus [15]. The dashed line shows the crossover from the nonaffine to the affine regime.

with α_m ($\propto G_{\text{eff}}$) from Fig. 2 demonstrates a remarkably accurate data collapse whose accuracy is enhanced as we move farther away from rigidity percolation. Moreover, we find that the same rescaling factor generates an equally accurate collapse of the K_{eff} data.

The collapse of our calculated elastic moduli with a single parameter, the length scale λ , is in good accord with the numerical data collapse found in previous simulations [5]. Thus, the mean-field theory demonstrates all previously observed mechanical signatures of the A-NA crossover. The analytic results, however, suggest $z \approx 1/4$, while the prior numerics pointed to $z = 1/3$. The dependence of the network mechanics on $\langle L \rangle / \lambda$ rather than entirely on $\langle L \rangle / R$ shows that the observed crossover is not governed by rigidity percolation [5]. The effective medium approach introduced here does not allow us to explore the spatial heterogeneities of the strain field under uniformly imposed shear, so it is impossible to explore the geometric interpretation of λ with this technique.

Although the effective medium approach is inexact and fails to account for the correct spatial structure of the strain field in the disordered material, it does show an abrupt crossover that appears mechanically identical to the A-NA crossover. The crossover is controlled by a single emergent length scale λ , which obeys a similar scaling relation to that found empirically from previous numerical results. From these G_{eff} plots (Fig. 4), we have extracted the A-NA crossover from the location of the largest change in the slope of the curves. This A-NA boundary is plotted in Fig. 3.

In conclusion, we used an effective medium theory to explore the mechanical properties of disordered filament networks. We find that this mean-field approach to the mechanics of such networks captures the mechanical as-

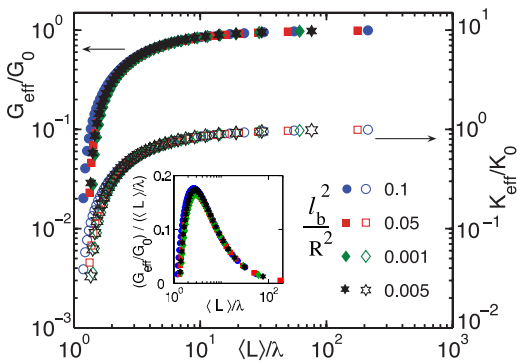


FIG. 4 (color online). The effective medium shear G_{eff}/G_0 (solid symbols) and bending K_{eff}/K_0 (open symbols) moduli normalized by their respective values in the infinite filament limit for a perfect network are plotted as a function of the mean filament length $\langle L \rangle$ divided by the nonaffinity length $\lambda = R/(R/l_b)^z$, with $z = 0.25$. The inset shows our method of locating the “knee” in G_{eff} as the peak in those curves. The data collapse is shown for four data sets differing in l_b as labeled in the legend.

pects of the A-NA crossover including the identification of an emergent mesoscopic length scale λ controlling the mechanics of the system.

M. D. and A. J. L. thank M. F. Thorpe, T. C. Lubensky, and E. Conti for useful discussions and acknowledge support from No. NSF-DMR0354113. F. C. M. acknowledges the hospitality of the UCLA chemistry department. This work was supported in part by the Foundation for Fundamental Research on Matter (FOM).

*Present address: Department of Physics and Astronomy, Vrije Universiteit, Amsterdam, The Netherlands.

- [1] M. Rubenstein and R. H. Colby, *Polymer Physics* (Oxford University, London, 2003).
- [2] P. A. Janmey, S. Hvidt, J. Lamb, and T. P. Stossel, *Nature* (London) **345**, 89 (1990); P. A. Janmey, *Curr. Opin. Cell Biol.* **3**, 4 (1991).
- [3] F. C. MacKintosh and P. A. Janmey, *Curr. Opin. Solid State Mater. Sci.* **2**, 350 (1997).
- [4] B. Alberts, D. Bray, J. Lewis, M. Raff, K. Roberts, and J. D. Watson, *Molecular Biology of the Cell* (Garland, New York, 1994), 3rd ed.
- [5] D. A. Head, A. J. Levine, and F. C. MacKintosh, *Phys. Rev. Lett.* **91**, 108102 (2003); D. A. Head, F. C. MacKintosh, and A. J. Levine, *Phys. Rev. E* **68**, 061907 (2003).
- [6] J. Wilhelm and E. Frey, *Phys. Rev. Lett.* **91**, 108103 (2003).
- [7] M. L. Gardel, J. H. Shin, F. C. MacKintosh, L. Mahadevan, P. A. Matsudaira, and D. A. Weitz, *Phys. Rev. Lett.* **93**, 188102 (2004); M. L. Gardel, J. H. Shin, F. C. MacKintosh, L. Mahadevan, P. Matsudaira, and D. A. Weitz, *Science* **304**, 1301 (2004).
- [8] J. Liu, G. H. Koenderink, K. E. Kasza, F. C. MacKintosh, and D. A. Weitz, *Phys. Rev. Lett.* **98**, 198304 (2007).
- [9] F. C. MacKintosh, J. Käs, and P. A. Janmey, *Phys. Rev. Lett.* **75**, 4425 (1995).
- [10] S. Feng, M. F. Thorpe, and E. Garboczi, *Phys. Rev. B* **31**, 276 (1985); L. M. Schwartz, S. Feng, M. F. Thorpe, and P. N. Sen, *Phys. Rev. B* **32**, 4607 (1985).
- [11] The mean distance between cross-links is always slightly greater than R due to missing cross-linking filaments in sparse networks. Corrections to the mean distance between cross-links grow as $(1-p)^4$.
- [12] M. Latva-Kokko and J. Timonen, *Phys. Rev. E* **64**, 066117 (2001); M. Latva-Kokko, J. Mäkinen, and J. Timonen, *Phys. Rev. E* **63**, 046113 (2001).
- [13] D. A. Head, F. C. MacKintosh, and A. J. Levine, *Phys. Rev. E* **68**, 025101 (2003).
- [14] The distinction between the two regions below the rigidity percolation line, which together constitute a solution phase, is likely to be unphysical. The new phase above this line corresponds within the mean-field approximation to a harmonic network without bond-bending forces.
- [15] When compared to previous work [12,13], the apparent shift of the rigidity percolation point to lower values of L/R is likely to be due to some combination of differing network connectivity and filament polydispersity.